Mid-Pleistocene Revolution and the ‘eccentricity myth’

Mark A. Maslin

Environmental Change Research Centre, Department of Geography, University College London, 26 Bedford Way, London, WC1H 0AP, UK

(e-mail:mmaslin@geog.ucl.ac.uk)

Andy J. Ridgwell

Department of Earth and Ocean Sciences, The University of British Columbia, 6339 Stores Road, Vancouver, British Columbia V6T 1Z4, Canada

Corresponding author M.A.Maslin

No of words = 5,800 (including abstract)

No of references = 46

No of Figures = 13

Abstract:

The mid-Pleistocene revolution (MPR) is the term used to describe the transition between 41 ky and 100 kyr glacial-interglacial cycles which occurred about one million years ago. Despite eccentricity having by far the weakest influence on insolation received at the Earth’s surface of any of the orbital parameters; it is often assumed to be the primary driver of the post MPR 100 kyr climate cycles. The traditional solution to this is to call for a highly nonlinear response by the global climate system to eccentricity. This ‘eccentricity myth’ is a simplified view of the relationship between global climate and orbital forcing and is in part due to an artefact of spectral analysis. Our aim here is to clarify the often confused role of eccentricity and review current theories of the MPR. We suggest the post-MPR ‘100 kyr’ glacial-interglacial cycles are more closely linked to precession, with the saw-toothed climate cycles being defined by every four or five precessional cycle. Because the control over the number of precessional cycles involved is determined by eccentricity, eccentricity at most only paces rather than drives the system. If true, then one must also question whether the MPR, itself defined by an abrupt change in spectral characteristics, is not also somewhat misconceived.

Background

The mid-Pleistocene transition or revolution (MPR) is the last major ‘event’ in a secular trend towards more intensive global glaciation that characterizes the last few tens of millions of years. The earliest recorded onset of significant global glaciation during the Cenozoic (65 Ma to present) was the widespread continental glaciation of Antarctica at about 34 Ma (e.g., Zachos *et al.* 2001). Glaciation in the Northern Hemisphere lagged behind, with the earliest recorded glaciation anywhere in the Northern Hemisphere occurring at between 10 and 6 Ma (e.g., Wolf-Welling *et al.* 1995). Subsequent marked expansion of continental ice sheets in the Northern Hemisphere was the culmination of long-term high latitude cooling, which began with this Late Miocene glaciation of Greenland and the Arctic and continued through to the major increases in global ice volume around 2.5 Ma (Maslin *et al.* 1998). This intensification of Northern Hemisphere glaciation seems to have occurred in three key steps: a) the Eurasian Arctic and Northeast Asia were glaciated at c. 2.75 Ma, b) glaciation of Alaska at 2.70 Ma, and c) the significant glaciation of the North East American continent at 2.54 Ma (Maslin *et al.* 2001). The extent of glaciation did not evolve smoothly after this, but instead was characterized by periodic advances and retreats of ice sheets on a hemispherical scale – the ‘glacial-interglacial cycles’.

The MPR is the term used to denote both the marked prolongation and intensification of these glacial-interglacial climate cycles that was initiated between 900 and 650 ka (e.g., Maasch & Saltzman, 1990; Berger & Jansen 1994; Mudelsee & Stattegger 1997). Since the onset of Northern Hemisphere glaciation at c. 2.75 Ma and prior to the MPR, global climate conditions appear to have primarily responded to the obliquity orbital periodicity (Imbrie et al. 1992). The consequences of this are glacial-interglacial cycles with a mean period of 41 kyr. After about 800 ka, glacial-interglacial cycles occur with a much longer mean period; approximately 100 kyr. Not only does the periodicity of glacial-interglacial cycles increase going through the MPR, but there is also an increase in the amplitude of global ice volume variations. The ice volume increase may in part be attributed to the prolonging of glacial periods and thus of ice accumulation. Evidence of this is provided by high-resolution oxygen isotope data from deep sea cores (Pisias & Moore 1981; Prell 1984; Shackleton *et al.* 1988; Tiedemann *et al.* 1994; Berger & Jansen 1994; Raymo *et al.* 1997; Mudelsee & Stattegger 1997). The amplitude of ice volume variation is also accentuated by the extreme warmth of many of the post-MPR interglacial periods; similar interglacial conditions can only be found at ~1.1 Ma, ~1.3 Ma and before ~2.2 Ma (Fig. 1). The MPR therefore marks a dramatic sharpening of the contrast between warm and cold periods. Mudelsee & Stattegger (1997) used advanced methods of time-series analysis to review deep-sea evidence spanning the MPR and summarized the salient features (Fig. 2). They suggest that the first transition occurs between 940 and 890 ka when there is a significant increase in global ice volume. However, the dominance of a 41 kyr climate response continues in their analysis. This two-state situation persists until about 650-725 ka when the climate system finds a three-state solution and the strong 100 kyr climate cycles begin (Mudelsee & Stattegger 1997). These three states correspond to; full interglacial conditions, the mild glacial conditions characteristic of Marine (oxygen) Isotope Stage (MIS) 3 and maximum glacial condition characteristic of MIS 2, i.e., the Last Glacial Maximum (LGM), a scheme developed by Paillard (1998).

The aim of this review is to clarify the often confused role of eccentricity in Quaternary climate variability. As the post MPR ‘100 kyr climates cycles’ have occasionally in the wider literature simply been attributed to eccentricity forcing, ‘the eccentricity myth’. However, as we will demonstrate the climate system response to orbital forcing is more complicated, with eccentricity providing the pacing rather than the driving force. It is therefore advantageous for palaeoclimatologists working on the Pleistocene to understand the current debates and consensus concerning the cause of the MPR, to allow them to better interpret their own climatic reconstructions. In order to develop this deeper understand the MPR and assess possible causes of the switch from 41 kyr to 100 kyr, we first need to review the 100 kyr glacial-interglacial cycles themselves.

The Glacial-Interglacial cycles

The oscillation between glacial and interglacial climates, which is the most fundamental environmental characteristic of the Quaternary Period, is believed to be primarily forced by changes in the Earth’s orbital parameters (Hays *et al.* 1976). However, one cannot assume there to be a direct cause-and-effect relationship between climate cycles and the Earth’s orbital parameters. This is because of the dominant effect of feedback mechanisms internal to the Earth’s climate system, which we will discuss later. An illustration of this is that the insolation received at the critical latitude of 65°N was the same 18 thousand years ago during the Last Glacial Maximum (LGM) as it is today (Laskar 1990; Berger & Loutre 1991).

There are three main orbital parameters, eccentricity, obliquity (tilt) and precession.

Eccentricity (Fig. 3a)

The shape of the Earth’s orbit changes from near circular to an ellipse over a period of about 100 kyr with a long cycle of about 400 kyr (in detail there are spectral peaks at 96, 125, and 413 kyr). Described another way the long axis of the ellipse varies in length over time. Today, the Earth is at its closest (146 million km) to the Sun on January 3rd: this position is known as perihelion. On July 4th the Earth is at its greatest distance from the Sun (156 million km) at the aphelion. Changes in eccentricity cause only very minor variations, approximately 0.03%, in the total annual insolation, but can have significant seasonal effects. If the orbit of the Earth were perfectly circular there would be no seasonal variation in solar insolation. Today, the average amount of radiation received by the Earth at perihelion is ~ 351 Wm^2 reducing to 329 Wm^2 at aphelion, a difference of more than 6%. At times of maximum eccentricity over the last 5 Myr this difference could have been as large as 30%. Because the intensity of solar radiation reaching the Earth diminishes as the square of the planet’s distance, global insolation falls at the present time by nearly 7% between January and July. This situation is more favourable for snow surviving in the Northern rather than Southern Hemisphere. The more elliptical the shape of the orbit becomes, the more the season will be exaggerated in one hemisphere and moderated in the other. The other effect of eccentricity is to modulate the precession effects (see below).

Obliquity (Fig. 3b)

The tilt of the Earth’s axis of rotation with respect to the plane of its orbit (the plane of the ecliptic) varies between 21.8˚ and 24.4˚ over a period of 41 kyr. It is the tilt of the axis of rotation that gives us the seasons. Because in summer the hemisphere is tilted towards the Sun, it is warmer because it receives more than 12 hours of sunlight and the Sun is higher in the sky. At the same time the opposite hemisphere is tilted away from the Sun and is colder because it receives less than 12 hours of sunlight and the Sun is lower in the sky. This hemisphere consequently is in winter. Hence, the greater the obliquity, the greater the difference between summer and winter.

Precession (Fig. 4)

There are two components of precession: one relating to the elliptical orbit of the Earth and the other relating to its axis of rotation. The Earth’s rotational axis moves around a full circle, or precesses, every 27 kyr (Fig. 4a). This is similar to the gyrations of the rotational axis of a toy spinning top. Precession causes the dates of the equinoxes to travel around the Sun resulting in a change in the Earth-Sun distance for any particular date, for example Northern Hemisphere summer (Fig. 4c). In addition there is the precession of the Earth’s orbit (Fig. 4b), which has a periodicity of 105 kyr and changes the time of year when the Earth is closest to the Sun (perihelion).

It is the combination of the different orbital parameters that results in the classically quoted precessional periodicities of 23 and 19 kyr. Combining the precession of the axis of rotation plus the precessional changes in orbit produces a period of 23 kyr. Combining the shape of the orbit i.e., eccentricity, and the precession of the axis of rotation results in a period of 19 kyr. These two periodicities combine so that perihelion coincides with the summer season in each hemisphere on average every 21.7 kyr, resulting in the precession of the equinoxes.

Combining eccentricity, obliquity and precession (Fig. 5)

Combining the effects of eccentricity, obliquity and precession provides the means of calculating the insolation for any latitude through time (e.g., Laskar 1990; Berger & Loutre 1991). Milankovitch (1949, translated 1969) suggested that summer insolation at 65˚N was critical in controlling glacial-interglacial cycles. He argued that if this summer insolation was reduced sufficiently then ice could survive through the summer and thus start to build-up eventually producing an ice sheet. Orbital forcing does have a large influence on this summer insolation. The maximum change in solar radiation in the last 600 kyr (see Fig. 5) is equivalent to reducing the amount of summer radiation received today at 65˚N to that received now over 550 km to the north at 77˚N. This in simplistic terms brings the present glacial limit in mid-Norway down to the latitude of Scotland. These lows in 65˚N insolation are caused by eccentricity enlongating the summer Earth-Sun distance, obliquity being shallow and precession placing the summer season at the longest Earth-Sun distance produced by eccentricity. It should also be noted that each of the orbital parameters has a different effect with changing latitude. For example the relative influence of obliquity increases the higher the latitude, whereas precession has its greatest influence in the tropics. Though as we will see later in this paper even at 65˚N precession is still the dominant influence on solar insolation received (e.g., Berger & Loutre, 1991; 1999). This is important when investigating different forcing functions.

Orbital inclination

For completeness, it is worth mentioning that a fourth possible orbital parameter has been identified – orbital inclination. It represents the variation in the angle of the Earth’s plane of orbit compared to the average orbit of the solar system (Farley and Paterson 1995; Muller & MacDonald 1997). This parameter has a period of 100 kyr, matching that observed in palaeoclimatic records. It has thus been argued that this might have changed the total amount of radiation received and could cause the Earth to pass through increased amounts of dust from outer space (Interplanetary Dust Particles, IDPs) which would encourage glacial-interglacial alternations with a

100 kyr periodicity. However, it is difficult to envisage how this could exert a direct influence on ice ages on Earth (Mudelsee & Schulz 1997; Kortenkamp & McDermott 1998; Paul & Berger, 1999), at least not with the correct phase.

Feedback mechanisms

Milankovitch (1949) initially suggested that the critical factor was total summer insolation at about 65˚N; because for an ice sheet to grow some additional ice must survive each successive summer. In contrast, the Southern Hemisphere is limited in its response because the expansion of ice sheets is curtailed by the Southern Ocean around Antarctica. The conventional view of glaciation is thus that low summer insolation in the temperate North Hemisphere allows ice to survive summer and thus starts to build-up on the northern continents (see detailed references in Maslin *et al.* 2001). If so, how then do we account for the MPR? Despite the pronounced change in Earth system response evidenced in palaeoclimatic records, the frequency and amplitude characteristics of the orbital parameters which force long-term global climate change, e.g., eccentricity (~100 kyr), obliquity (~41 kyr) and precession (~21 and ~19 kyr), do not vary during the MPR (Berger & Loutre 1991, 1999). This suggests that the cause of change in response at the MPR is internal rather than external to the global climate system. This brings us the role of ‘feedbacks’ in the glacial-interglacial cycles.

Orbital forcing in itself is insufficient to drive the observed glacial-interglacial variability in climate. Instead, the Earth system amplifies and transforms the changes in insolation received at the Earth’s surface through various feedback mechanisms. As snow and ice accumulate due to initial changes in insolation regime, the ambient environment is modified. This is primarily by an increase in albedo, and with it a reduction in the absorption efficiency of incident solar radiation, and thus a suppression of local temperatures. This will promote the accumulation of more snow and ice and thus a further modification of the ambient environment, etc. – the classic ‘ice albedo’ feedback (Fig. 6).

Another feedback is triggered when the ice sheets, particularly the Laurentide ice sheet on North America, become big enough to deflect the atmospheric planetary waves. This changes the storm path across the North Atlantic Ocean and prevents the Gulf Stream and North Atlantic Drift penetration as far north as today. This surface ocean change combined with the general increase in melt-water in the Nordic Seas and Atlantic Ocean due to the presence of large continental ice sheet ultimately leads to reduces the production of deep water. This in turn reduces the amount of warm water pulled northwards. All of which leads to increased cooling in the Northern Hemisphere and expansion of the ice sheets (see detailed references in Maslin *et al.* 2001).

However, the action of these and similar ‘physical climate’ feedbacks on variations in solar insolation received at the Earth’s surface is not sufficient to allow a complete accounting of the timing and magnitude of the glacial-interglacial cycles, at least post-MPR. There is mounting evidence that other feedback mechanisms may be equally, if not more important in driving the long-term climate system. The role of ‘greenhouse’ gases in the atmosphere that absorb outgoing infrared radiation is critical (e.g., Berger 1988; Saltzman, & Maasch, 1988; Maasch and Saltzman, 1990; Saltzman, & Maasch, 1991; Saltzman *et al.* 1993; Berger & Loutre 1993; Li et al. 1998). Any reduction in the atmospheric concentration of atmospheric constituents such as CO_2, CH_4 and water vapour will drive a general global cooling (Fig. 6), which in turn furthers glaciation. We already know that these properties varied considerably over the glacial-interglacial cycles. For CO_2 and CH_4 this variability is recorded in air bubbles trapped in polar ice (Petit *et al.* 1999) and is coeval with changes in global ice volume (Shackleton 2000; Ruddiman and Raymo 2003). Glacial periods are by their very nature drier which reduces atmospheric water vapour, and Lea *et al.* (2000) provide clear evidence that water vapour production of the equatorial Pacific zone was greatly curtailed during the last five glacial periods. The importance of greenhouse gases is illustrated by the improved spectral characteristics of climate model response. For instance, the observed single sharp peak corresponding to a period of ~100 kyr rather than the split fingerprint of eccentricity is invariably not replicated without observed changes in atmospheric CO_2 being taken into account (e.g., Ridgwell *et al.* 1999).

Feedbacks are also central to the climate system’s exit from glaciation. Deglaciation turns out to be much quicker than glaciation because of the natural instability of ice sheets (Maslin *et al.* 2001). In the case of the last deglacation or Termination I, the transition from glacial to interglacial state lasted a maximum of only 4 kyr, even including the brief return to glacial conditions called the Younger Dryas period (see detailed references in Maslin *et al.* 2001). Two controls are operating. 1) increase in summer 65°N insolation (e.g., Imbrie et al. 1993) which provides melting forcing on the Northern Hemisphere ice sheets and tendency to retreat, and 2) the rise of atmospheric carbon dioxide and methane which promotes warming globally and encourages the melting of the large continental ice sheets (Shackleton 2000; Ruddiman & Raymo 2003). With a sufficient initial rise in sea level, large ice sheets adjacent to the oceans will be undercut, which in turns increases sea level. This sea-level feedback mechanism can be extremely rapid. Once the ice sheets are in retreat then the other feedback mechanisms discussed for glaciation are thrown into reverse (Fig. 6). These feedbacks are prevented from becoming a run away affect by the limit of how much heat the North Atlantic can steal from the South Atlantic to maintain the interglacial deep water overturning rate and a limit on the amount of carbon that can be exported into the atmosphere. What is interesting is that these mechanisms for rapid deglaciation produce a saw-tooth climate signal which is characteristic of glacial-interglacial cycles post-MPR.

Potential causes of the MPR

If the action of powerful feedbacks within the Earth system are central to the main characteristics of the post-MPR ‘100 kyr’ glacial-interglacial cycles such as the rapid and complete deglaciation events, then one might deduce that the behaviour of the Earth system prior to the MPR must presumably involve a much weaker action or absence of these ‘100 kyr’ deglaciation feedbacks. The MPR can thus be viewed as a change from a linear (Imbrie *et al.* 1992) to a non-linear forced climate system (Imbrie *et al.* 1993). Many different hypotheses have been postulated to produce this critical non-linear transition which we review briefly below.

a) Critical size of the Northern Hemisphere ice sheets:

Imbrie *et al.* (1993) suggested that the Northern Hemisphere ice sheets may have reached a critical size during the MPR allowing them to respond non-linearly to eccentricity. One suggested way of producing a transition in ice sheet size is through erosion of regolith beneath the Laurentide ice sheet (Clark & Pollard 1998). In this view, once sufficient regolith has been eroded with the periodic 41 kyr advance and retreat of the earlier glacial cycles, the ice sheet would start to rest directly on bed rock, enabling it to take on an equilibrium form with a much greater height. Because much more ice mass can now be accumulated than before, the ice sheet can survive longer than the 41 kyr driving force.

b) Global cooling trend

It has been suggested that long term cooling through the Cenozoic instigated a threshold which allowed the ice sheets to become large enough to ignore the 41 kyr orbital forcing and to survive between 80 and 100 ka (Abe-Ouchi 1996; Raymo et al. 1997). In one version of this, Gildor & Tziperman (2000) and Tziperman & Gildor (2003) suggest that long term cooling of the deep ocean during the Pleistocene alters the relationship between atmospheric temperature and accumulation rates of snow on continental ice sheets and the growth of sea ice. They envision this alteration causing more extensive global coverage of sea ice. The climate could then be affected by a so-called sea-ice switch which would produce the rapid asymmetric deglaciation observed after the MPR.

c) The global carbon cycle and atmospheric CO_2

One way of driving a cooling trend as discussed above is, of course, to reduce the concentration of greenhouse gases in the atmosphere. A secular decline in the concentration of CO_2 in the atmosphere through the late Cenozoic could have brought the global climate to a threshold, allowing it to respond non-linearly to orbital forcing thereafter (Mudelsee and Stattegger 1997; Mudelsee and Schultz 1997; Raymo et al. 1997; Berger et al. 1999). Saltzman (2001) takes this further and proposes that in crossing this threshold (‘bifurcation’) an internal instability arises in the global carbon cycle that leads to the activation of an internal 100 kyr oscillator. In this view, orbital forcing plays only a very minor phase-locking role.

If atmospheric carbon dioxide and not Northern Hemisphere ice volume is the primary driving force of the ~100 kyr glacial-interglacial cycles, then an interpretation consistent with palaeoclimatic proxies suggests that eccentricity, atmospheric carbon dioxide, Vostok (Antarctica) air temperatures and deep water temperatures are in phase; whereas ice volume lags these other variables (Shackleton 2000). In this case the MPR could represent a change in the internal response of the global carbon cycle to orbital forcing. However, what caused the secular decline in atmospheric CO_2 and what precise changes in the global carbon cycle gave rise to the observed CO_2 variability is still an open question (Archer *et al.* 2000). For the latter, suspicion currently rests on the Southern Ocean as one of the most important regions modulating atmospheric carbon dioxide over the glacial-interglacial cycles (Sigman & Boyle 2000; Ridgwell *et al.* 2003).

d) Greenland-Scotland submarine ridge

Denton (2000) envisioned a MPR mechanism based on the uplift of the Greenland-Scotland submarine ridge at about 950 ka. This was caused by a surge of tectonic activity along the Iceland mantle plume, and ultimately led to a southward shift of the area of deep-water production from the Arctic to the Nordic seas. This would have had a number of further effects on oceanic circulation, especially during times of expanded ice sheets, so that once ice-sheet expansion had commenced, it became much more difficult for the thermohaline conveyor to re-set into an interglacial mode. In other words, after 950 ka, it became easier for ocean circulation to lock into a glacial rather than interglacial mode.

e) Intermediate ocean circulation and gas hydrates

Kennett *et al.* (2003) suggest that at the MPR there was a re-organisation of the ocean circulation at intermediate water depth. This would have allowed warmer intermediate water to occur only during periods of significant changes such as deglaciations. This warmer water would have caused the destabilization of gas hydrates on the continental shelves and slopes and thus the release of methane. This additional atmospheric methane would have enhanced global warming, accelerated the deglaciation and hence causing the sharp saw-toothed pattern observed for the last eight glacial-interglacial cycles.

The ‘eccentricity myth’

The major problem with understanding the MPR is how to interpret the ‘100 kyr’ glacial-interglacial cycles and the role of eccentricity. There are two primary views. The first suggest that there is non-linear amplification in the climate system of the eccentricity signal, the second is that the other orbital parameters drive global climate change and eccentricity rather acts as a pacing mechanism. In the wider palaeoclimatic community we believe this debate has not received the attention that it should, and in many cases the last eight glacial-interglacial cycles are thought to be synomous with ‘eccentricity forcing’. This view or ‘myth’ is fundamentally flawed and prevents many excellent palaeoclimatic records from being interpreted correctly.

Below we demonstrate why eccentricity can not be the direct forcing of the 100 kyr glacial-interglacial cycles.

Eccentricity has spectral peaks at 95 kyr, 125 kyr and 400 kyr (Fig. 7). In contrast, the spectral analysis of benthic foraminiferal oxygen isotopes (Fig. 7a or 8a) which are a proxy for global ice volume, consistently reveals a single peak that dominates the spectra lying very close to a period of 100 kyr (Muller & MacDonald 1997) (Figs 7b and 9b). If eccentricity were the primary cause of the 100 kyr cycle then one would expect the global ice volume ~100 kyr spectral peak to contain a double peak and that there would be at least some power at 400 kyr (Fig. 7b and 9c) (Ghil & LeTreut 1981; Muller & MacDonald 1997; Berger 1999). Ruddiman (2003) for instance clearly shows that the maximum of either an interglacial or glacial is missed by a simple 100,000 year filter (Fig. 10).

This mismatch between the spectral signatures has led to the search for alternative drivers for the assumed ‘pure’ 100 kyr response of the climate system, such as the orbital inclination driver proposed by Muller & MacDonald (1997). However, a strong 100 kyr spectral peak in a truncated time series does not imply the presence of a 100 kyr periodicity in the data. Indeed, Ridgwell *et al.* (1999) showed that the observed spectral signature of ice volume can be reproduced by a simple saw-tooth pattern based on the long glaciation period followed by the short deglaciation (Figs 8c and 9d). Here, the timing of the rapid deglaciation event is simply assumed to occur synchronous with every fourth or fifth precessional cycle. A similar saw tooth pattern can also be produced from obliquity using every second or third cycle, but the spectral analysis of this parameter matches the global ice volume signal less precisely (Fig. 9e). The length of the glacial-interglacial cycles is far from uniform in this analysis, differing in duration by a complete precessional cycle (21 kyr). The resultant spectral signature with a dominant ‘100 kyr’ peak this thus in effect an artefact of spectral analysis applied to this sort of data, and does not imply the presence of a strong cycle frequency in the artificial data. The unevenness in the observed data is clear if the duration of the last seven glacial periods are compared using ‘untuned’ sediment core $\delta^{18}O$ records (Raymo 1997). Figure 11 shows that the time between deglaciations can vary from 119 kyr to as little as 87 kyr over the last 700 ka. Although the deglacial transitions are no more than quasi-periodic and do not recur at anything like a regular 100 kyr interval, the results of spectral analysis of the rather limited c. 600-800 kyr data set gives the appearance of a ~100 kyr periodicity present in the data. This is the ‘eccentricity myth’.

The possibility that eccentricity is the primary forcing of the post MPR 100 kyr cycles is also brought into doubt by the Stage 11 Paradox (e.g., Berger & Wefer 2003; Droxler *et al.* 2003). The Marine Oxygen Isotope Stage (MOIS) 11 Paradox is this: the amplitude of the climate variability between the glacial MOIS 12 and interglacial MOIS 11 (c. 420 ka) is at a maximum at the very time when astronomical forcing is at minimum. Eccentricity longer cycle is approximately 400 kyr, so at present and during Stage 11 eccentricity forcing and thus precession is at a minimum (Berger & Wefer 2003).

We therefore suggest that a direct forcing role for eccentricity in the post-MPR glacial-interglacial cycles is not a conclusion that can be robustly drawn from the results of spectral analysis, nor the climate records. Instead, the influence of precession seems to be critical. Raymo (1997) suggested that the episodic occurrence of unusually low maxima in Northern Hemisphere summer insolation is the critical factor controlling subsequent deglaciation. In this model, glacial termination only occurs when the climate system has been predisposed by excessive ice sheet growth by a previous low maxima in Northern Hemisphere summer insolation to some critical maximum degree of glaciation. Of course one such time is the LGM. This critical threshold might reflect the sinking of the underlying bedrock to an extent sufficient to allow full activation of additional and catastrophic mechanisms of ice sheet collapse once the ice sheet starts to initially retreat under an unfavourable combined insolation and CO_2 radiative forcing regime. In other words, precession driven summer minima push the glacial climate system too far and it collapses all the way back into an interglacial period. Although eccentricity (and obliquity) determines the envelope of precessional amplitude and thus ultimately whether the minimum occurs on the fourth or fifth precessional cycle, the MPR still does not represent the onset of nonlinear amplification of eccentricity to any meaningful interpretation of ‘nonlinear’.

The nature of the MPR

Prior to the MPR the climate system was sensitive to obliquity-forced latitudinal insolation gradients which exerted a strong control on summer atmospheric heat transport. Although the insolation curves for the Northern Hemisphere are dominated through time by precession, the insolation gradient between high and low latitude is dominated by obliquity. This obliquity driven high- to low-latitude insolation gradient must therefore be the prime control on glacial-interglacial cycles prior to the MPR. Raymo & Nisancioglu (2003) suggest that differential heating between high and low latitudes controls the atmospheric meridional flux of heat, moisture and latent heat which exerts a dominant control on global climate. This is because the majority of heat transport between 30˚ and 70˚N is by the atmosphere: thus a linear relationship between obliquity, northward heat transport and glacial-interglacial cycles can be envisioned. When this summer heat transport was low the ice sheets could build-up, and when this heat transport increased the ice sheets correspondingly shrunk. This is a bi-modal system responding linearly to increases and decreases in northward heat transport. The limited size of continental ice sheets meant they were less susceptible to rapid deglaciation due to sea level rise, promoting the observed relatively gradual deglaciations. The spectral signature of ice volume therefore reflects a dominance of obliquity and precession.

In contrast, following the MPR, the cyclicity in ice volume is dominated by the prominent quasi-periodic rapid deglaciation events. Ruddiman (2003; 2004) recently characterized this system by considering the role of all three orbital parameters and their respective influence on greenhouse gases and continental ice sheets (Fig. 12). When linear forcings from obliquity are applied to atmospheric CO_2 and ice volume, and from precession to atmospheric CO_2, CH_4, and ice volume then there are periods when these re-enforce each other to produce deep glacial maximums and rapid deglaciations (Fig. 13). The classic spectral signature of the post-MPR world with the prominent ‘100 kyr’ peak does not arise because the ice sheets no longer respond to precession and obliquity. Indeed, one might predict from the Ruddiman model that the higher frequency portion of the spectrum would remain similar across the MPR, which is borne out by the data. Rather than a reduction in the absolute importance of the higher frequencies, it is the introduction of the quasi-periodicity of the deglacial transitions to the previously precessional and obliquity-dominated spectrum that gives rise to the observed change in spectral characteristics.

The nature of the MPR is therefore not the introduction of a high degree of nonlinear amplification of eccentricity, but the achievement of a system state that allows ice sheets to survive during weak precession insolation maxima and grow large enough during obliquity ice volume maxima to generate a strong positive CO_2

feedback (Ruddiman 2003; 2004). The deglacial transitions are primed by the occurrence of a prior anomalous precessional insolation regime and global ice volume above some critical threshold, and dominate the form of the post-MPR glacial-interglacial cycles. The MPR can therefore be thought of as representing the first time that a new, deeper glacial state is achievable. This deeper glacial state might be enabled by the introduction of a strong positive CO_2 feedback with ice volume, for instance (Ruddiman 2003; 2004). Such a scenario would be consistent with recent speculations regarding the role of 'iron fertilization' of the ocean biota, and feedbacks with CO_2, climate, and aeolian delivery of iron (Ridgwell & Watson 2002; Ridgwell 2003). A secular trend in global cooling is equivalent to the effects of a long-term drawdown of atmospheric CO_2, also supporting a critical role for the global carbon cycle in the MPR. The question of the MPR might then be reduced to understanding the variability in atmospheric CO_2 over the past few millions years, rather than ice volume *per se*. Unfortunately, we still do not fully understand the reasons for the variability in CO_2 observed in ice core records, or even the magnitude of the minimum at the LGM (Archer *et al.* 2000; Ridgwell *et al.* 2003). Furthermore, the longest that current ice core CO_2 records reach back is 420 kyr (Petit *et al.* 1999), far short of the MPR. Although it is possible that data currently being analysed from the EPICA core drilled on Dome C (Wolff 2002; EPICA 2004) may extend back far enough to shed new light on the MPR, our incomplete understanding of past carbon cycling may prove a hindrance for some time yet.

A new perspective on the MPR

If the post-MPR '100 kyr' cycles are in effect an artefact of the spectral analysis of a truncated time series containing a dominant quasi-periodic glacial termination motif, then one must also question what we really mean by the 'mid-Pleistocene Revolution'. Although there is a clear visible change in the appearance of the ice volume variability revealed in proxy records (e.g., Fig. 11), the MPR is typically defined through spectral analysis. The results of evolutive spectral analysis studies suggest an abrupt change in dominant frequency and mean ice volume associated with the MPR, although not necessarily occurring synchronously (e.g., Mudelsee & Schulz 1997; Mudelsee & Stattegger 1997). The implications are of an abrupt shift to a new mode (oscillation) of the climate system, or 'bifurcation'. However, it is less easy to see this elegant picture from the raw data. For instance, whereas arguably the first ‘100 kyr’ like glacial-interglacial cycle occurs at c. 950 ka (MOIS 23 to 22) and is immediately followed by a second at c. 860 ka (MOIS 21 to 20), there occurs between 780 and 620 ka (MOIS 19-16) an interval of apparent obliquity-dominated variability in ice volume (Fig. 11). Even between 620 ka (MIOS 16) and present, the variability in ice volume at times more closely resembles the pre-MPR 41 kyr ‘world’ and there is a failure to fully achieve the ice volume maximum and subsequent prominent deglacial transition. However, despite visual inspection of the data suggesting that there is no entirely reliable re-occurrence of the ‘100 kyr’ motif after the MPR, there seems to be sufficient quasi-periodic recurrence contained in the past 600 or 900 kyr to imply a much more clear-cut transition in the spectral analysis.

The MPR could be thought of not as a transition to a new mode of glacial-interglacial cycles *per se*, but simply the point at which a more intense and prolonged glacial state and associated subsequent rapid deglaciation becomes possible. An important point in this view is that whereas from the MPR onwards it may be possible for the climate system to achieve this new glacial climate solution, it need not do each time. The success or failure to achieve this state would be determined by factors such as the exact details of insolation regime and carbon cycling. One would also expect an increasing probability of a ‘100 kyr’ motif occurring with time, as the long-term late Cenozoic cooling/CO_2 trend presumably continues. The lack of a sufficient evolving stochastic element in the climate system could help explain why the model of Paillard (1998) predicts the continued recurrence of a ‘100 kyr’ motif once first initiated, which results in a much earlier onset of a strong 100 kyr spectral peak than the data contain. In the data, the 100 kyr peak only ‘appears’ in the evolutive spectrum once there is sufficient quasi-periodic recurrence of the ‘100 kyr’ motif within the moving 500 kyr window (Paillard 1998).

One implication is that the MPR thus defined, could actually precede the first visible sign of an anomalous climatic occurrence although whether viewing the MPR in this way is particularly useful is another matter. However, the lesson to be drawn from the ‘eccentricity myth’ is that delineating the MPR as the appearance of ‘100 kyr’ cyclicity with spectral analysis is potentially misleading, and could hinder identification and interaction of the underlying mechanisms involved in the Earth system.

Acknowledgements
We would like to thank Martin Head for inviting us to the one day conference on ‘Early/Middle Pleistocene Transitions’ at Cambridge University. We would like to thank Bill Ruddiman and André Paul for the detailed and extremely helpful comments. We would like to acknowledge all the help of the UCL Department of Geography Drawing Office in help in preparing the diagrams for this paper.

References

Abe-Ouchi, A. 1996. Quaternary transition: A bifurcation in forced ice sheet oscillations? Eos Transactions AGU, 77 (46), Fall Meeting Supplement, F415.

Berger, A. 1988. Milankovitch Theory of Climate. Review of Geophysics, 26(4), 624-657.

Berger, A. & Loutre, M. F. 1991. Insolation values for the climate of the last 10 million years. Quaternary Science Reviews, 10, 297-317.

Berger, A. & Loutre, M. F. 1996. Modelling the climate response to the astronomical and CO2 forcing. Comptes Rendus de l’Academie des Sciences de Paris, 323, series IIa, 1-16.

Berger, A., Li, X., Loutre, MF. 1999. Modelling northern hemisphere ice volume over the last 3 Ma. Quaternary Science Reviews, 18, 1-11.

Berger, W. H. 1999. The 100-kyr ice-age cycle: internal oscillation or inclinational forcing? International Journal Earth Science, 88, 305-316.

Berger, W. H. & Jansen, E. 1994. Mid-Pleistocene climate shift: the Nansen connection. In: Johannessen *et al.* (eds). The polar oceans and their role in shaping the global environment. AGU Geophysical Monograph 85, 295-311.

Berger, W. H., Bickert, T., Schmidt, H. & Wefer, G. 1993. Quaternary oxygen isotope record of pelagic foraminiferas: Site 806, Ontong Java Plateau. In: Berger, W.H., Kroenke, L.W., Mayer, L.A. *et al.*, Procedings ODP, Scientific Results, 130, College Station, TX (Ocean Drilling Program), 381-395.

Berger, W. H. & Wefer G. 1996. Expeditions into the Past: Paleoceanographic studies in the South Atlantic, In: Wefer *et al.* (editors) The South Atlantic: present and past ciculation, Spinger-Verlag, Berlin, 363-410.

Berger, W. H. & Wefer, G. 2003. On the dynamics of the ice ages: Stage-11 paradox, mid-Brunhes climate shift and 100-ky cycle. In: Droxler, A., Poore, R. & Burckle, L. (eds) Earth's Climate and Orbital Eccentricity: The Marine Isotope Stage 11 Question, Geophysical Monograph Series 137, 41-59.

Clark, P. & Pollard, D. 1998. Origin of the middle Pleistocene transition by ice sheet erosion of regolith. Paleoceanography, 13, 1-9.

Denton, G. H., 2000. Does asymmetric thermohaline-ice-sheet oscillator drive 100,000-yr cycles, Journal of Quaternary Science, 15, 301-318.

Droxler, A., Poore, R. & Burckle, L. 2003. Earth's Climate and Orbital Eccentricity: The Marine Isotope Stage 11 Question, Geophysical Monograph Series 137, p.240.

EPICA community members. 2004. Eight glacial cycles from an Antarctic ice core. Nature, 429, 623-628.

Farley, K. & Patterson, D. B. 1995. A 100 kyr periodicity in the flux of extraterrestrial ^{3}He to the sea floor. Nature, 378, 600-603.

Gildor, H. & Triperman, E. 2000. Sea ice as the glacial cycles climate switch, Paleoceanography, 15, 605-615.

Hays, J.D., Imbrie, J. & Shackleton, N.J. 1976. Variations in the Earth's orbit: Pacemaker of the Ice Ages. Science, 194, 1121-1132.

Imbrie, J., Berger, A., Boyle, E. A., Clemens, S. C., Duffy, A., Howard, W. A., Kukla, G., Kutzbach, J., Martinson, D. G., McIntyre, A., Mix, A. C., Molfino, B., Morley, J. J., Peterson, L. C., Pisias, N. G., Prell, W. G., Raymo, M. E., Shackleton, N. J. & Toggweiler, J. R. 1993. On the structure and origin of major glaciation cycles. 2. The 100,000 year cycle. Paleoceanography 8, 699-735.

Imbrie, J., Boyle, E., Clemens, S., Duffy, A., Howard, W., Kukla, G., Kutzbach, J., Martinson, D., McIntyre, A., Mix, A., Molfino, B., Morley, J., Peterson, L., Pisias, N., Prell, W., Raymo, M., Shackleton, N. & Toggweiler, J. R. 1992. One the structure and origin of major glaciation cycles. 1. Linear responses to Milankovitch forcing. Paleoceanography, 7, 701-738.

Kennett, J., Cannariato, K.G., Hendy, I.L. & Behl, R.J. 2003. Methane hydrates in Quaternary climate change: The clathrate gun hypothesis: American Geophysical Union, p.216.

Kortenkamp, S. J., & Dermott, S. F. 1998. A 100,000 year periodicity in the accretion rate of interplanetary dust. Science, 280, 874-876.

Laskar, J. 1990. The chaotic motion of the solar system: A numerical estimate of the chaotic zones. Icarus, 88, 266-291.

Lea, D.W., Pak, D., & Spero, H. 2000. Climate impact of late Quaternary equatorial sea surface temperature variations. Science, 289, 1719-1724.

Li, X.S., Bergerm A., & M.F. Loutre, 1998. CO_2 and Northern Hemisphere ice volume variations over the middle and late Quaternary. Climate Dynamic, 14, 537-544.

Maasch, K. A. & Saltzman, B. 1990. A low-order dynamical model of global climatic variability over the full Pleistocene. Journal of Geophysical Research, 95, 1955-1963.

Maslin M.A., Li, X. S., Loutre M. F., & Berger A. 1998. The contribution of orbital forcing to the progressive intensification of Northern Hemisphere Glaciation. Quaternary Science Reviews, 17, 411-426.

Maslin, M.A., Seidov, D. & Lowe, J. 2001. Synthesis of the nature and causes of sudden climate transitions during the Quaternary In: Seidov, D. Haupt B., & Maslin, M. A. eds) The oceans and rapid climate change: past, present and future AGU Geophysical Monograph Series 126, 9-52.

Milankovitch, M.M. 1949. Kanon der Erdbestrahlung und seine Anwendung auf das Eiszeitenproblem. Royal Serbian Sciences, Spec. pub. 132, Section of Mathematical and Natural Sciences, 33, Belgrade, p.633 (Canon of Insolation and the Ice Age Problem, English translation by Israel Program for Scientific Translation and published for the U.S. Department of Commerce and the National Science Foundation, Washington D.C., 1969).

Mudelsee, M. & Schulz, M. 1997. The Mid-Pleistocene climate transition: onset of 100 ka cycle lags ice volume build up by 280 ka. Earth and Planetary Science Letters, 151, 117-123.

Mudelsee, M. & Stattegger, K. 1997. Exploring the structure of the mid-Pleistocene revolution with advance methods of time-series analysis. Geologische Rundschau, 86, 499-511.

Muller, R. A. & MacDonald, G. J. 1997. Glacial cycles and astronomical forcing. Science 277, 215-218.

Paillard, D. 1998. The timing of Pleistocene glaciations from a simple multiple-state climate model. Nature, 391, 378-381.

Paul, A. & W. H. Berger W. H. 1999. Climate cycles and climate transitions as a response to astronomical and CO_2 forcings. In Harff, J.,Lemke, W. &

Stattegger, K. (eds) Computerized modeling of sedimentary Systems. Springer-Verlag, Berlin, Heidelberg, 223-245.

Petit, J. R., Jouzel, J., Raynaud, D., Barkov, N., Barnola, J., Basile, I., Bender, M., Chappellaz, J., Davis, M., Delaygue, G., Delmotte, M., Kotlyakov, V., Legrand, M., Lipenkov, V., Lorius, C., Pepin, L., Ritz, C., Saltzman, E. & Stievenard, M. 1999. Climate and atmospheric history of the Past 420 000 years from the Vostok Ice Core, Antarctica. Nature, 399, 429-436.

Pisias N.G. & Mooore, T.C. 1981. The evolution of Pleistocene climate: a time series approach. Earth Planet, 52, 450-458.

Prell, W. L. 1984. Covariance patterns of foraminifera $\delta^{18}O$: An evaluation of Pliocene ice-volume changes near 3.2 million years ago. Science, 226, 692-694.

Raymo, M. E. 1997. The timing of major climate terminations. Paleoceanography, 12, 577-585.

Raymo, M. E. & Nisancioglu, K. 2003. The 41 kyr world: Milankovitch’s other unsolved mystery, Paleoceanography, 18, 1, 1011, DOI: 10.1029/2002PA000791.

Raymo, M., Oppo, D. & Curry, W. 1997. The mid-Pleistocene climate transition: A deep sea carbon isotope perspective. Paleoceanography, 12, 546-559.

Ridgwell, A. & Watson, A. 2002. Feedback between aeolian dust, climate and atmospheric CO_2 in glacial times, Paleoceanography, 17(4), 1059, DOI 10.1029/2001PA000729.

Ridgwell, A., Watson, A. & Raymo, M. 1999. Is the spectral signature of the 100 kyr glacial cycle consistent with a Milankovitch origin. Paleoceanography, 14, 437-440.

Ridgwell, A. J., Watson, A. J., Maslin, M. A. & Kaplan, J. O. 2003. Implications of coral reef build-up for the controls on atmospheric CO_2 since the Last Glacial Maximum. Palaeoceanography, 18(4), 1083 10.1029/2003PA000893.

Ruddiman, W. F. 2003. Orbital insolation, ice volume, and greenhouse gases. Quaternary Science Reviews, 22, 1597-1629.

Ruddiman, W. F. 2004. The role of greenhouse gases in orbital-scale climatic changes. EOS, 285, 1, 6-7.

Ruddiman, W.F. & Raymo, M.E. 2003. A methane-based time scale for Vostok ice. Quaternary Science Reviews, 22, 141-155.

Saltzman, B. 2001. Dynamical paleoclimatology : generalized theory of global climate change. Academic Press, San Diego, p.320.

Saltzman, B. & Maasch, K. A. 1988. Carbon cycle instability as a cause of the late Pleistocene ice age oscillations: modeling the asymmetric response. Global Biogeochemical Cycles, 2, 177--185.

Saltzman, B., & Maasch, K. A. 1991. A first-order global model of late Cenozoic climatic change. Climate Dynamics, 5, 201-210.

Saltzman, B., Maasch, K.A. & Verbitsky, M. Ya. 1993. Possible effects of anthropogenically increased CO_2 on the dynamics of climate: Implications for ice age cycles. Geophysical Research Letters, 20, 1051-1054.

Shackleton, N.J. 2000. The 100,000 year Ice Age cycle identified and found to lag temperature, carbon dioxide and orbital eccentricity. Science, 289, 1989-1902.

Shackleton, N.J., Imbrie, J. & Pisias, N.G. 1988. The evolution of oceanic oxygen-isotope variability in the North Atlantic over the past 3 million years. Philosophical Transactions of the Royal Society of London, B, 318, 679-686.

Sigman, D. & Boyle, E. 2000. Glacial/interglacial variations in atmospheric carbon dioxide. Nature, 407, 859 – 869.

Tiedemann, R., Sarnthein, M. & Shackleton, N.J. 1994. Astronomic timescale for the Pliocene Atlantic $\delta^{18}O$ and dust flux records of ODP Site 659. Paleoceanography, 9, 619-638.

Tziperman, E. & Gildor, H. 2003. On the mid-Pleistocene transition to 100 kyr glacial cycle and the asymmetry between glaciation and deglaciation times. Paleoceanography 18, 1, 1001, DOI: 10.1029/2001PA000627.

Wilson R.C.L. 2000. The Great Ice Age. Routledge, London, p.315.

Wolf-Welling, T.C.W., Thiede, J., Myhre, A.M. & Leg 151 Shipboard scientific party. 1995. Bulk sediment parameter and coarse fraction analysis: Paleoceanographic implications of Fram Strait Sites 908 and 909, ODP Leg 151 (NAAG), Eos Transactions, 76 (17), supplement, 166.

Wolff, E. 2002. Extending the ice core record beyond half a million years, EOS, Transactions of the American Geophysical Union, 83(45), 509.

Zachos, J.C., Pagani, M., Sloan, L., Thomas, E. & Billups, K. 2001. Trends, rhythms and aberrations in global climate 65 Ma to present. Science 292, 686-693.

Figure Captions

Fig. 1. Generalised planktonic and benthic foraminiferal oxygen isotope curves for the last 6 million years compared with the two main stages in the intensification of Northern Hemisphere glaciation.

Fig. 2. Detailed statistical analysis of the mid-Pleistocene revolution by Mudelsee & Stattegger (1997) demonstrating a delay of 200 kyr between a significant increase in global ice volume and the start of the 100 kyr glacial-interglacial cycles. They show that global ice volume increased significantly between 940 and 890 ka. Whereas evolutionary spectral analysis reveals an abrupt increase of 100-ka cycle amplitude much later at approximately 650 ka. Probability density function (PDF) exhibits a bifurcation behaviour at approximately 725 ka. This suggests that the MPR moved from two state system, full glacial period and full interglacial period to a more complicated system with multiple states as suggested by Paillard (1998) and Saltzman (2001).

Fig. 3. Changes in the shape of the Earth's orbit around the Sun. (a) The shape of the orbit changes from a near circular to elliptical. The position along the orbit when the Earth is closest to the Sun is termed the perihelion and the position when it is farthest from the Sun is the aphelion. (b) The present-day orbit and its relationship to the seasons, solstices and equinoxes (after Wilson *et al.* 2000).

Fig. 4. The components of the precession of the equinoxes. (a) The precession of the Earth's axis of rotation. (b) The precession of the Earth's orbit. (c) The precession of the equinoxes (after Wilson *et al.* 2000).

Fig. 5. Variations in the Earth's orbital parameters: eccentricity, obliquity and precession and the resultant Northern Hemisphere 65˚N insolation for the last half million years (after Wilson *et al.* 2000).

Fig. 6. Summary of the conventional view of the feedback mechanism forced by insolation at 65°N which drives glaciation and deglaciation. H = Heinrich events, LGM = Last Glacial Maximum, AB = Allerød-Bølling Interstadial, YD = Younger Dryas and D-O = Dansgaard-Oeschger cycles.

Fig. 7. a) general properties of benthic foraminifera oxygen isotope records from mainly the Pacific (OJsox96) and the Atlantic (Imb84) for the last 700 kyr (adapted from Berger *et al.* 1996). These provide an alternative to SPECMAP presented in Fig. 8. Marine oxygen isotope stages are labelled. b) fourier spectra of the two series, showing not the strong single peak at ~100 kyr, but the dominant orbital frequencies of 19, 23, 41, 95, 125 and 400 kyr.

Fig. 8. a) SPECMAP stacked $\delta^{18}O$ composite showing marine oxygen isotopes stage, b) insolation for June 21st 65˚N showing the quasi-periodic insolation maxima of unusually low strength (shown by arrows) preceding glacial –interglacial terminations by one precessional cycle in each case, and c) sawtooth artificial ice volume signal used in Figure 9 (adapted from Ridgwell *et al.* 1999).

Fig. 9. a) Spectral power signature of SPECMAP stacked $\delta^{18}O$ composite (see Figure 8) together with expanded low-frequency spectra of b) SPECMAP stacked $\delta^{18}O$ composite, c) orbital eccentricity, d) June 21st 65˚N insolation-based sawtooth see Figure 8, e) obliquity-based sawtooth, f) threshold-based model, and g) LLN 2-D model with orbital forcing and atmospheric carbon dioxide (adapted from Ridgwell *et al.* 1999).

Fig. 10. Ruddiman’s (2003) eloquent demonstration that a 100,000 year filter cannot capture the form of the climatic signals which contain both saw-toothed and square-wave shapes. Either the 100,000 year maximum or minimum is mismatched compared with the peak interglacial (IG) or glacial (G) maximum (adapted from Ruddiman 2003).

Fig. 11. Comparison of the benthic foraminiferal oxygen isotope curve from ODP Site 659 (Tiedemann *et al.* 1994) with the timing between Terminations. Timing back to Termination VII are taken from Raymo’s (1997) compilation. Older dates between Terminations have been taken directly from the Tiedemann *et al.* (1994) orbitally tuned oxygen isotope curve.

Fig. 12. Ruddiman’s (2003) assumption of linear forcing of obliquity on ice volume and atmospheric carbon dioxide and precession on ice volume and atmospheric carbon dioxide and methane compared with the ice volume signal for the last 200 kyr. Marine oxygen isotope stage shown.

Fig. 13. Ruddiman’s (2003) model of combined obliquity and precession forcings shown in Fig. 12 to produce the 100,000 year global ice volume signal. Precessional forcing produces the forcing towards interglacial states while obliquity produces the forcing towards glacial conditions.

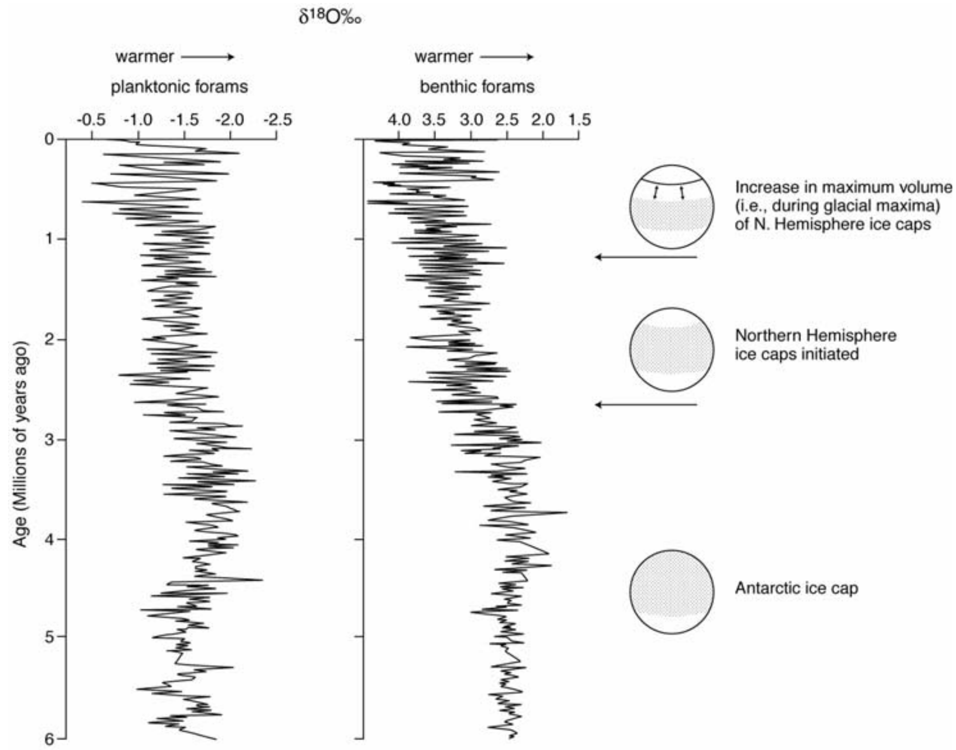
δ18O‰
warmer
planktonic forams
-0.5 -1.0 -1.5 -2.0 -2.5
warmer
benthic forams
4.0 3.5 3.0 2.5 2.0 1.5
Age (Millions of years ago)
0
1
2
3
4
5
6
Increase in maximum volume
(i.e., during glacial maxima)
of N. Hemisphere ice caps
Northern Hemisphere
ice caps initiated
Antarctic ice cap

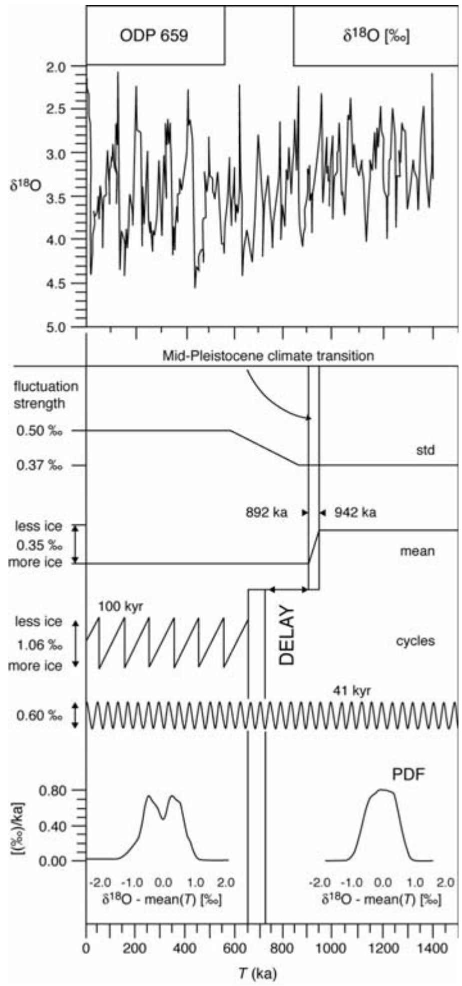

ODP 659
$\delta^{18}O$ [‰]
$\delta^{18}O$
Mid-Pleistocene climate transition
fluctuation strength
0.50 ‰
0.37 ‰
std
892 ka
942 ka
less ice
0.35 ‰
more ice
mean
100 kyr
less ice
1.06 ‰
more ice
DELAY
cycles
41 kyr
0.60 ‰
PDF
[(‰)/ka]
$\delta^{18}O$ - mean(T) [‰]
$\delta^{18}O$ - mean(T) [‰]
T (ka)

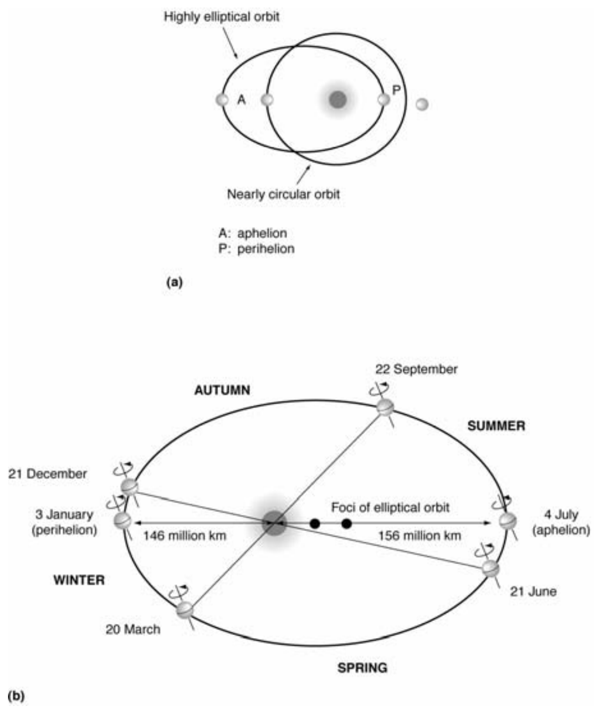
Highly elliptical orbit
A
P
Nearly circular orbit
A: aphelion
P: perihelion
(a)
22 September
AUTUMN
SUMMER
21 December
3 January
(perihelion)
Foci of elliptical orbit
4 July
(aphelion)
146 million km
156 million km
WINTER
21 June
20 March
SPRING
(b)

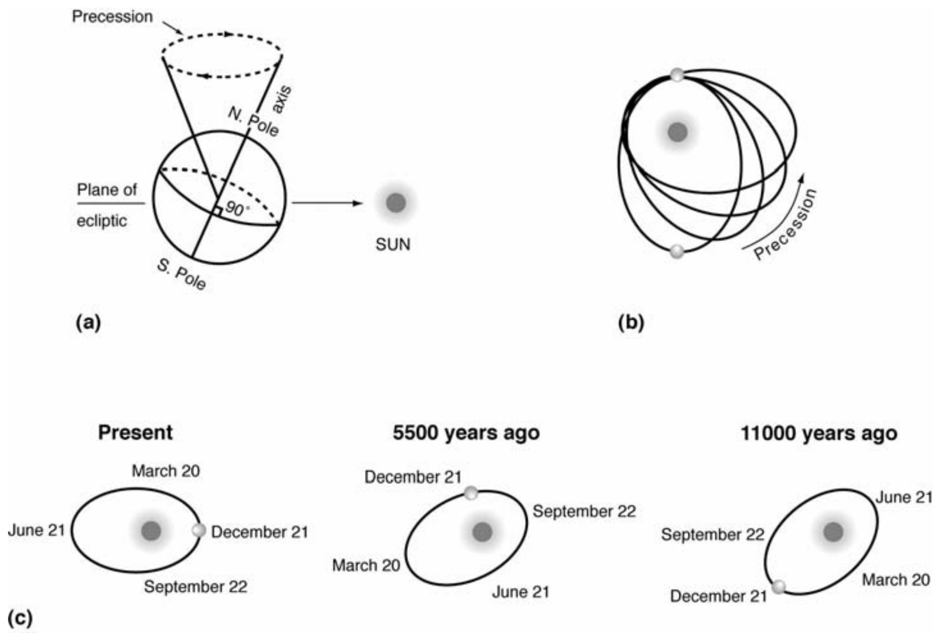
Precession
axis
N. Pole
Plane of
ecliptic
90°
SUN
S. Pole
(a)
Precession
(b)
Present
March 20
June 21
December 21
September 22
5500 years ago
December 21
September 22
March 20
June 21
11000 years ago
June 21
September 22
March 20
December 21
(c)

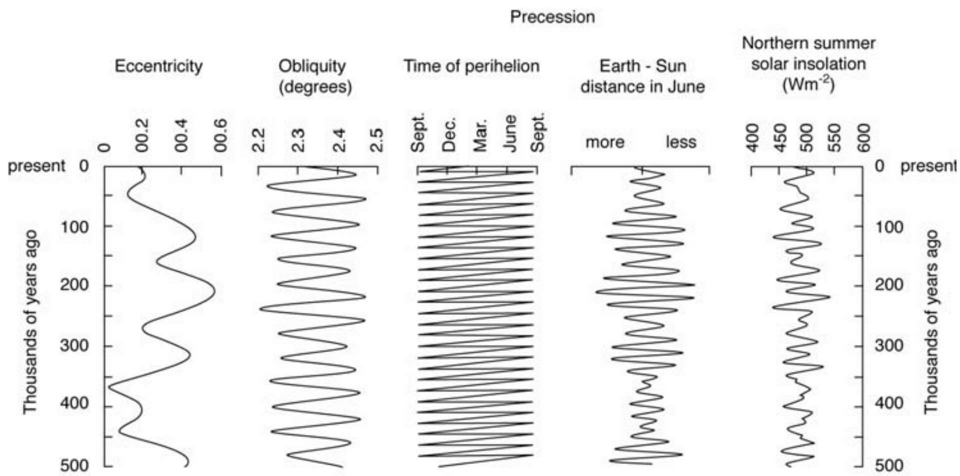
Precession
Eccentricity
Obliquity (degrees)
Time of perihelion
Earth - Sun distance in June
Northern summer solar insolation (Wm-2)
0
00.2
00.4
00.6
2.2
2.3
2.4
2.5
Sept.
Dec.
Mar.
June
Sept.
more
less
400
450
500
550
600
present 0
100
200
300
400
500
Thousands of years ago
0 present
100
200
300
400
500
Thousands of years ago

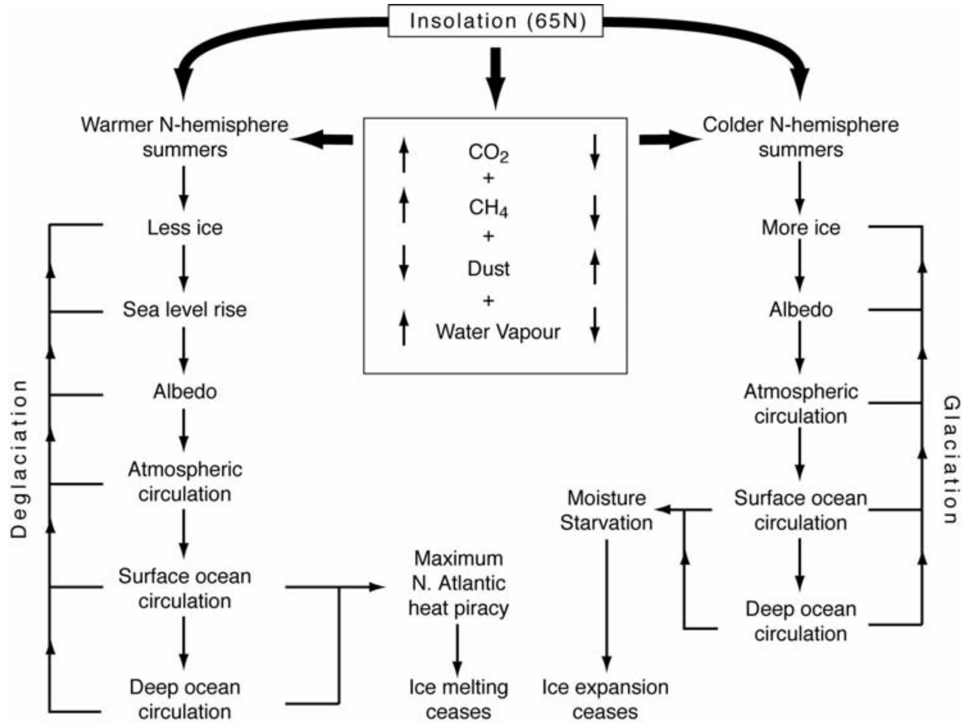
Insolation (65N)
Warmer N-hemisphere summers
Colder N-hemisphere summers
CO2
+
CH4
+
Dust
+
Water Vapour
Less ice
Sea level rise
Albedo
Atmospheric circulation
Surface ocean circulation
Deep ocean circulation
Deglaciation
More ice
Albedo
Atmospheric circulation
Surface ocean circulation
Deep ocean circulation
Glaciation
Moisture Starvation
Maximum N. Atlantic heat piracy
Ice melting ceases
Ice expansion ceases

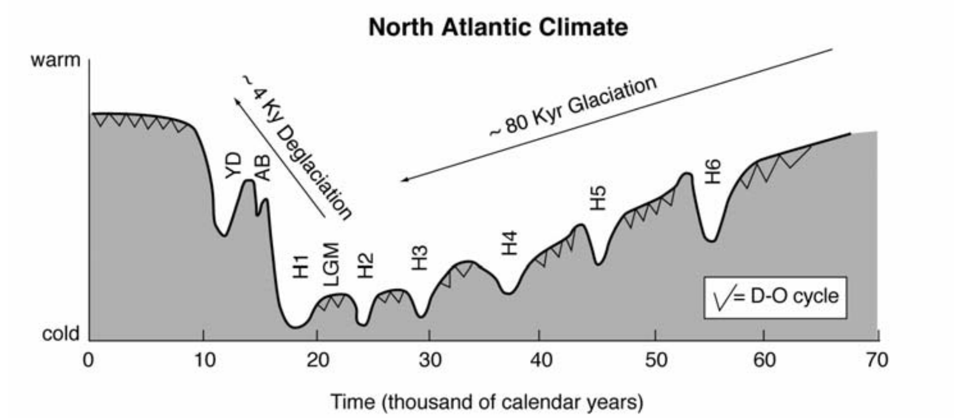
North Atlantic Climate
warm
cold
~ 4 Ky Deglaciation
~ 80 Kyr Glaciation
YD
AB
H1
LGM
H2
H3
H4
H5
H6
= D-O cycle
0
10
20
30
40
50
60
70
Time (thousand of calendar years)

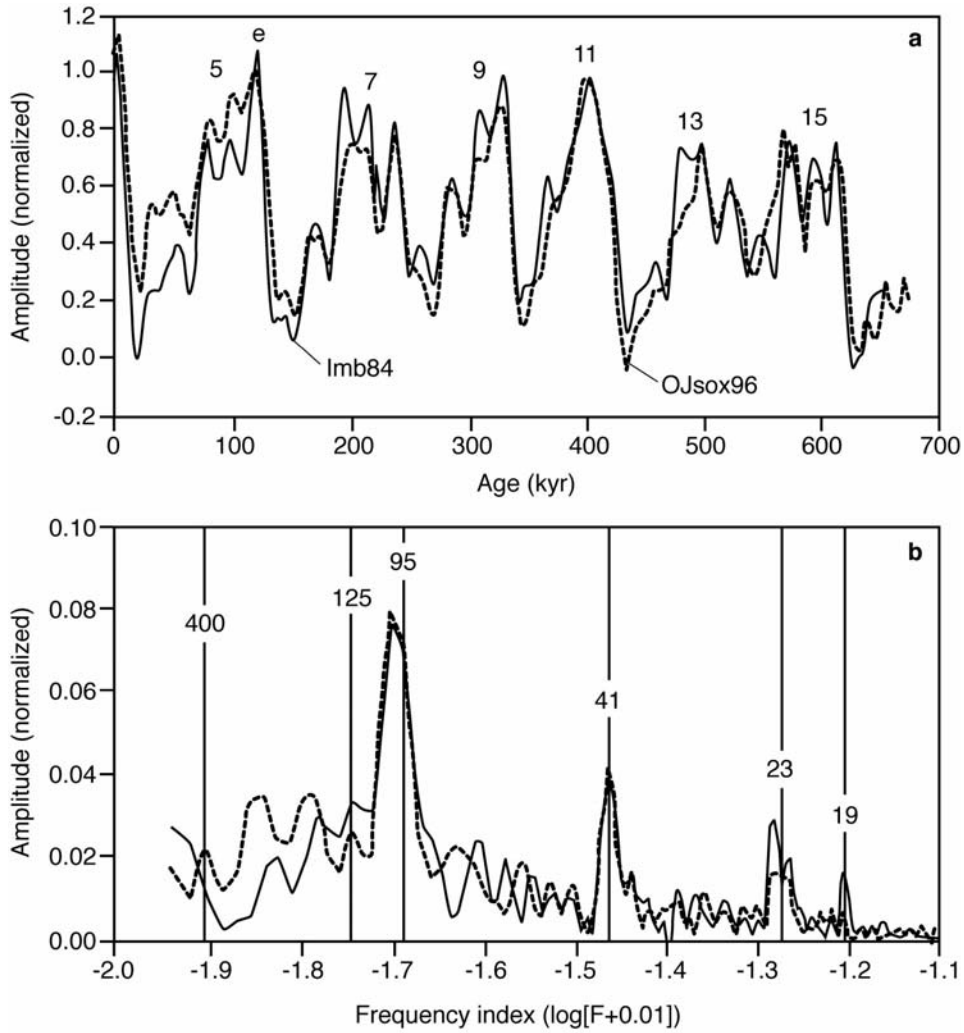
a
Amplitude (normalized)
Age (kyr)
e
5
7
9
11
13
15
Imb84
OJsox96
b
Frequency index (log[F+0.01])
400
125
95
41
23
19

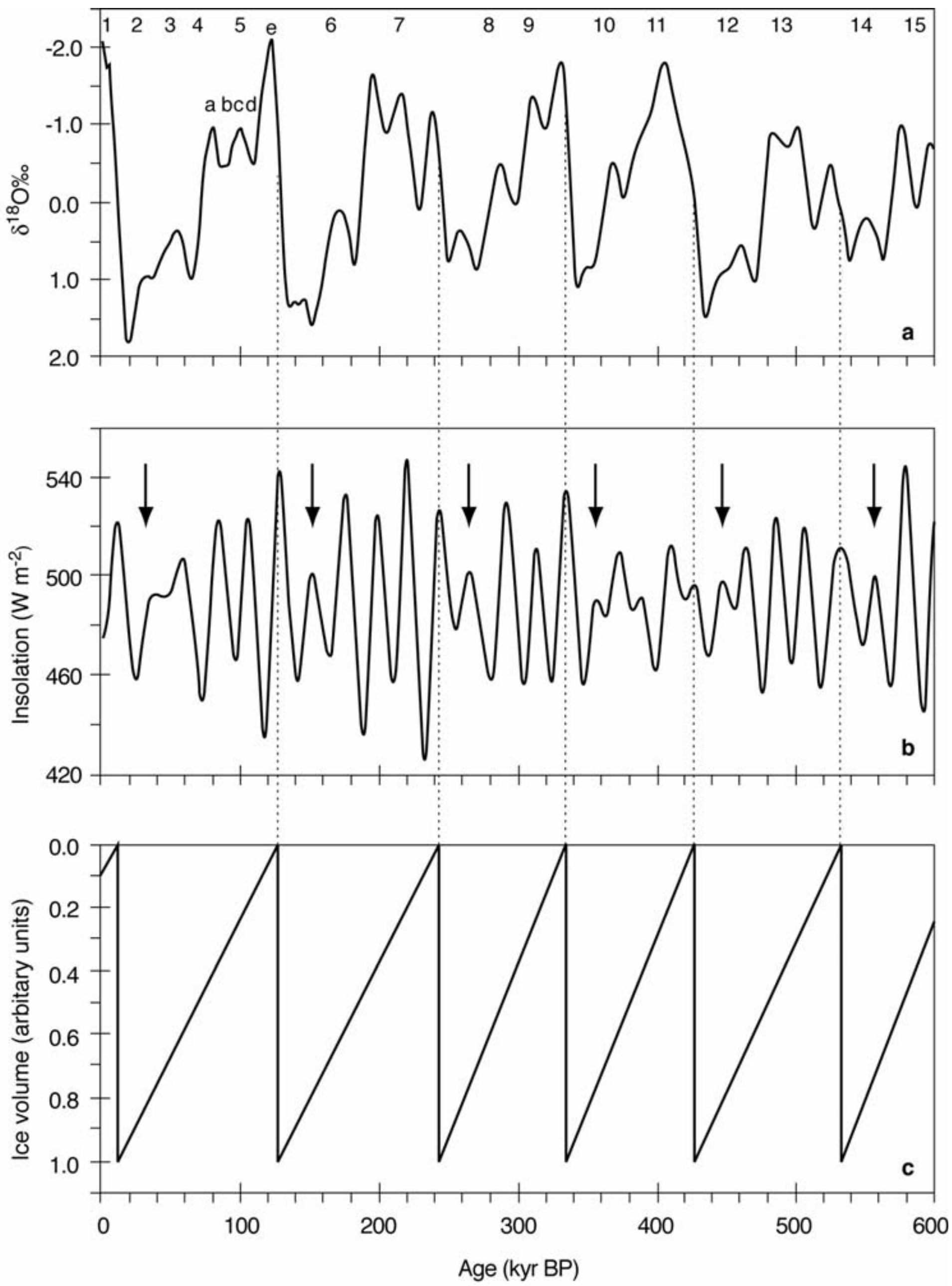
1 2 3 4 5 e 6 7 8 9 10 11 12 13 14 15
a bcd
δ18O‰
-2.0
-1.0
0.0
1.0
2.0
a
Insolation (W m-2)
540
500
460
420
b
Ice volume (arbitary units)
0.0
0.2
0.4
0.6
0.8
1.0
c
0
100
200
300
400
500
600
Age (kyr BP)

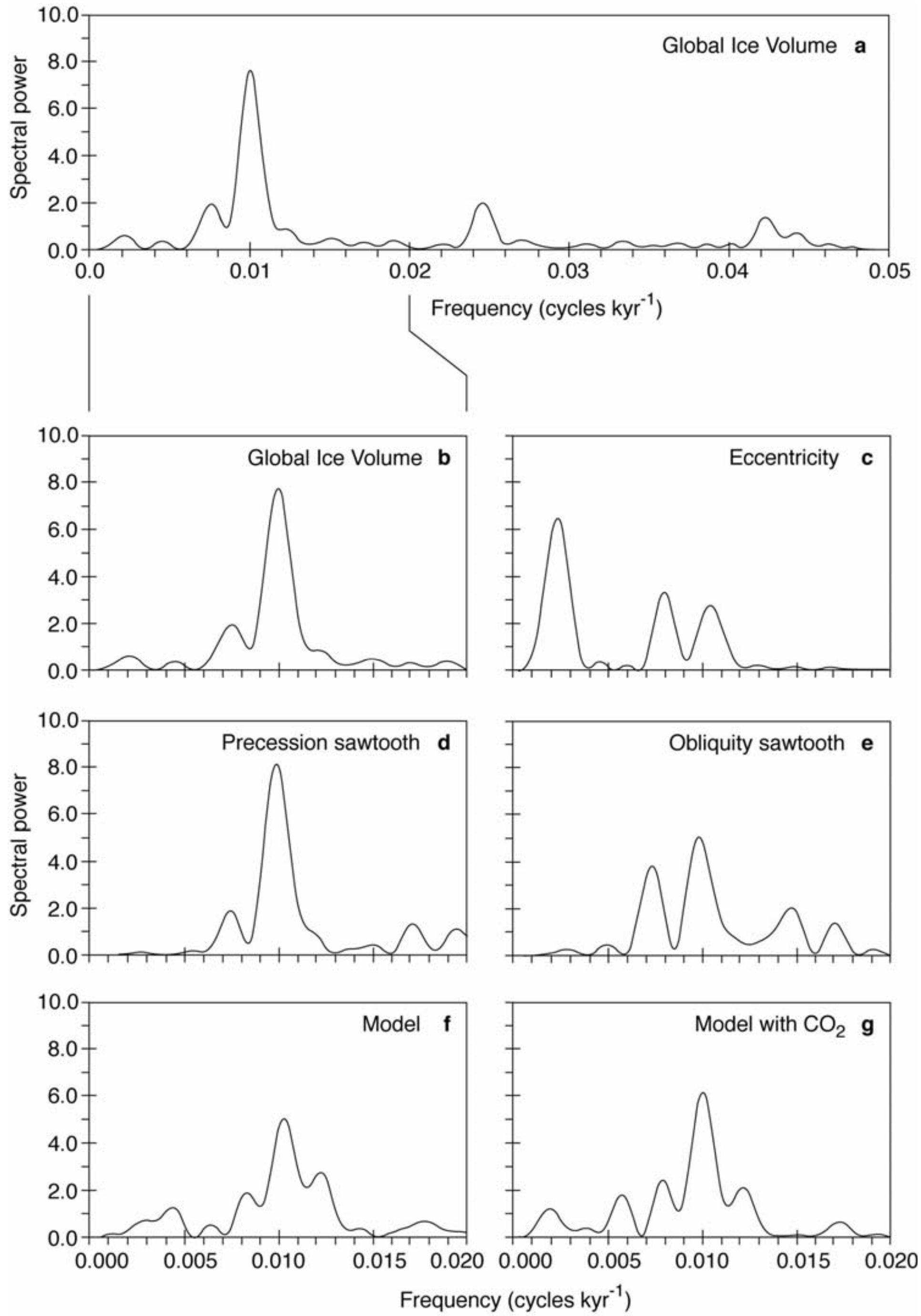
Global Ice Volume a
Spectral power
Frequency (cycles kyr-1)
Global Ice Volume b
Eccentricity c
Precession sawtooth d
Obliquity sawtooth e
Model f
Model with CO2 g

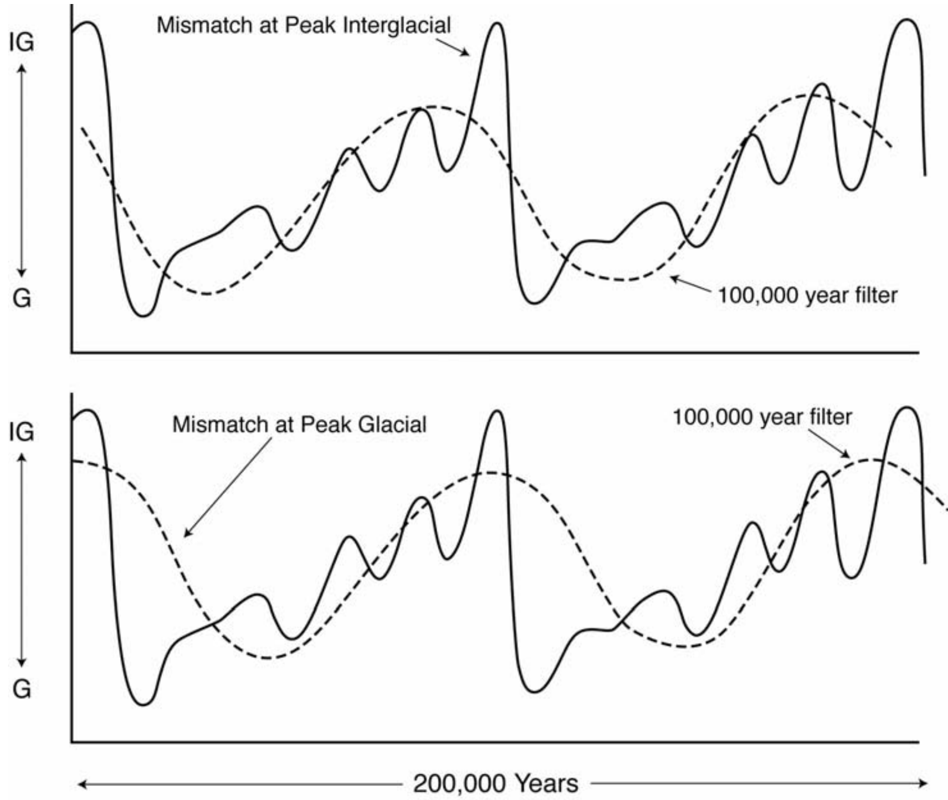
Mismatch at Peak Interglacial
IG
G
100,000 year filter
Mismatch at Peak Glacial
100,000 year filter
IG
G
200,000 Years

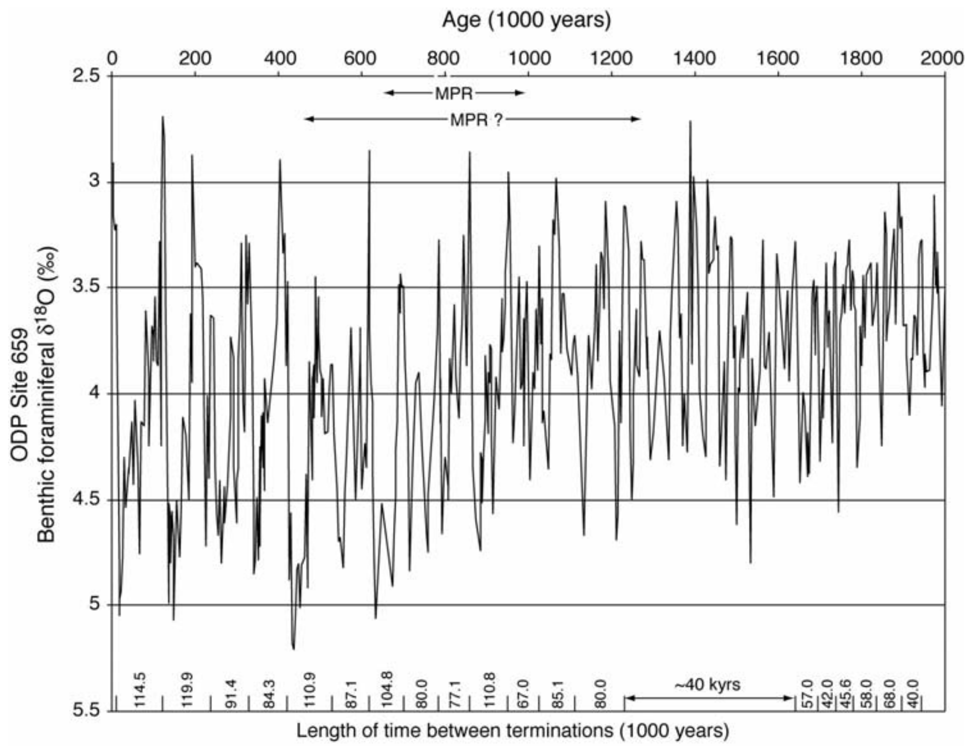
Age (1000 years)
0
200
400
600
800
1000
1200
1400
1600
1800
2000
MPR
MPR ?
ODP Site 659
Benthic foraminiferal δ18O (‰)
2.5
3
3.5
4
4.5
5
5.5
114.5
119.9
91.4
84.3
110.9
87.1
104.8
80.0
77.1
110.8
67.0
85.1
80.0
~40 kyrs
57.0
42.0
45.6
58.0
68.0
40.0
Length of time between terminations (1000 years)

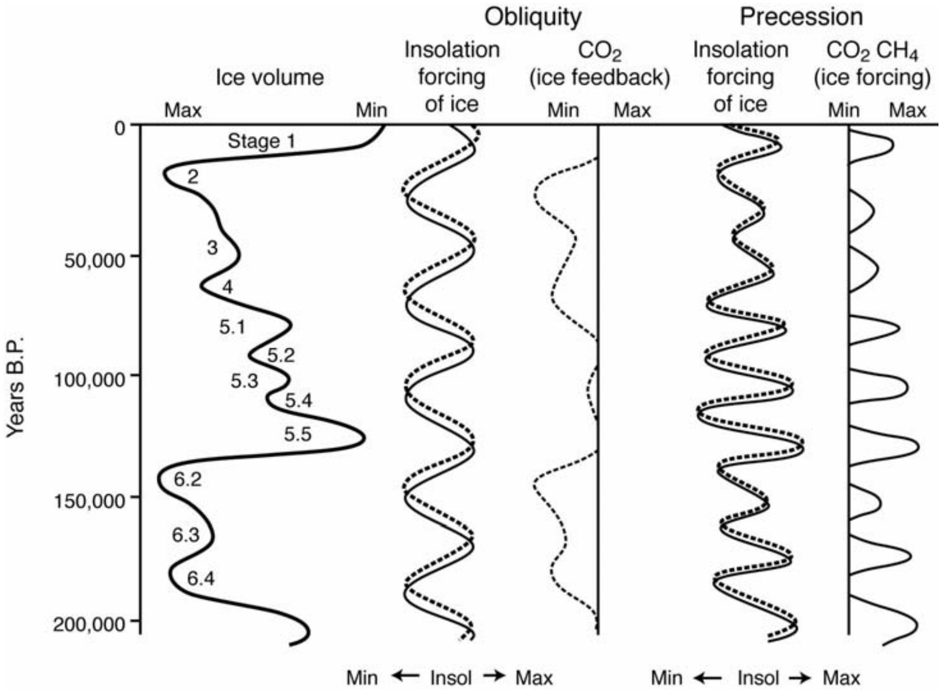
Obliquity
Precession
Ice volume
Insolation forcing of ice
CO2 (ice feedback)
Insolation forcing of ice
CO2 CH4 (ice forcing)
Max
Min
Min
Max
Min
Max
Stage 1
2
3
4
5.1
5.2
5.3
5.4
5.5
6.2
6.3
6.4
0
50,000
100,000
150,000
200,000
Years B.P.
Min ← Insol → Max
Min ← Insol → Max

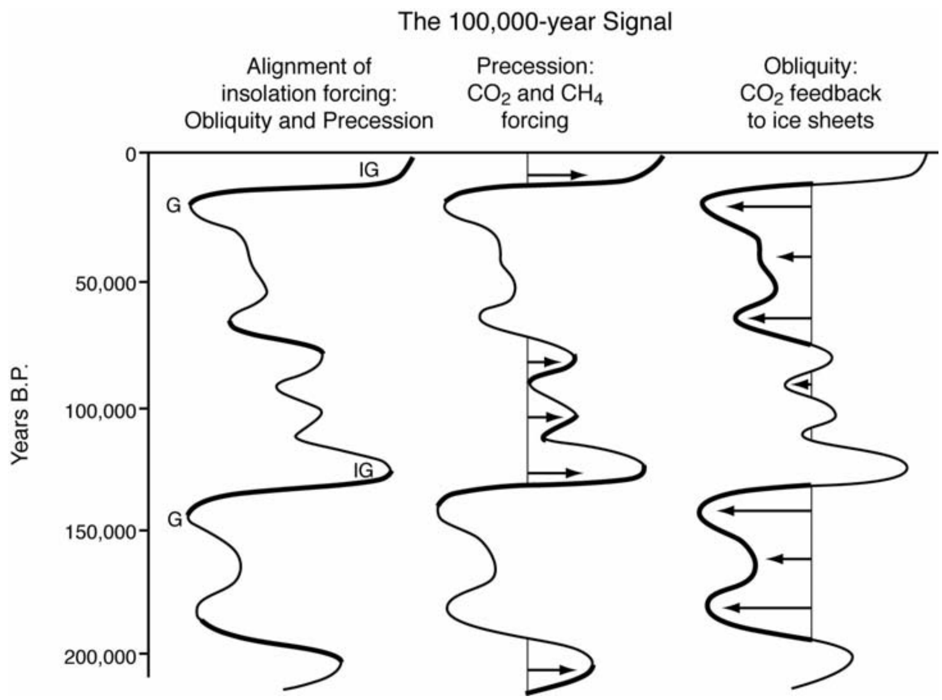
The 100,000-year Signal
Alignment of insolation forcing: Obliquity and Precession
Precession: CO2 and CH4 forcing
Obliquity: CO2 feedback to ice sheets
Years B.P.
0
50,000
100,000
150,000
200,000
IG
G
IG
G